ICSV13 - Vienna
The Thirteenth International Congress on Sound and Vibration
Vienna, Austria, July 2-6, 2006

NONLINEAR CHARACTERISTICS OF THE INTERNAL DAMPING OF COMPOSITE MATERIALS USED IN FLYWHEEL APPLICATIONS

Alfonso Moreira*, George T. Flowers

Department of Mechanical Engineering, Auburn University
201 Ross Hall, Auburn University, AL 36849-5341, USA
moreial@eng.auburn.edu

Abstract

An investigation of the nonlinear characteristics for the internal damping of graphite fibre-epoxy composite materials for use in flywheel components is presented. Special attention is given to the dependence of vibration damping on the displacement amplitude and natural frequency of the test samples. These samples consisted of thin composite beams held in a clamping fixture that allows one of the ends to be adjusted, stretching the sample so as to vary the first natural frequency. The characteristics of a series of transient vibration responses at the first natural frequency obtained experimentally were studied, showing a clear relationship between the amplitude of vibration at each frequency and the associated damping. Linear and nonlinear lumped-parameter system models were developed and evaluated for accuracy and functionality. These models of vibration damping can be implemented in complex models for flywheel systems simulation in order to enhance the reliability and accuracy of the predicted vibration stability thresholds.

INTRODUCTION

Flywheel energy storage systems for aerospace application require materials that have high strength and low weight. In the search for materials to build components for such, composite materials and, especially, fibre reinforced composites, are a popular choice. They offer a wide range of tailoring possibilities, light weight, and can withstand very high stress levels.

Extensive research has been conducted to determine the damping characteristics of composite materials [3] [4]. These works include the consideration of viscous and hysteretic damping as well as nonlinear effects. In addition, the influence of internal damping as a driver for rotordynamic instability has received attention from various authors (references). These works have included both simplified and detailed studies and have considered both modelling/analysis and experimental testing. However, a practical model for analyzing the dynamic behaviour of flexible composite rotor components that accounts for changes in effective damping ratio with vibration amplitude and natural frequency is not currently available.

Although the dependence of damping ratio on vibration displacement is widely recognized, there has been little work that has employed the method of free vibrations to assess such dependence [2]. As can be seen in Figure 1a, a single (unique) value for the damping ratio does not adequately represent the actual shape of an experimentally measured vibration decay rate. Figure 1b (where the vertical axis is represented by log scale) illustrates further the dramatic differences between the damping ratios at low and high amplitudes. As the displacement amplitude of the vibration increases, the value of the damping ratio increases as well. In dynamic systems, where stability can be highly dependent on internal damping, such increase may shift the *effective* stability thresholds considerably for some designs. Accordingly, the objective of this paper is to assess the functional form of the amplitude dependence of damping ratio for carbon-epoxy composites in order to improve the predictive capability of dynamic models of speed flywheel energy storage systems.

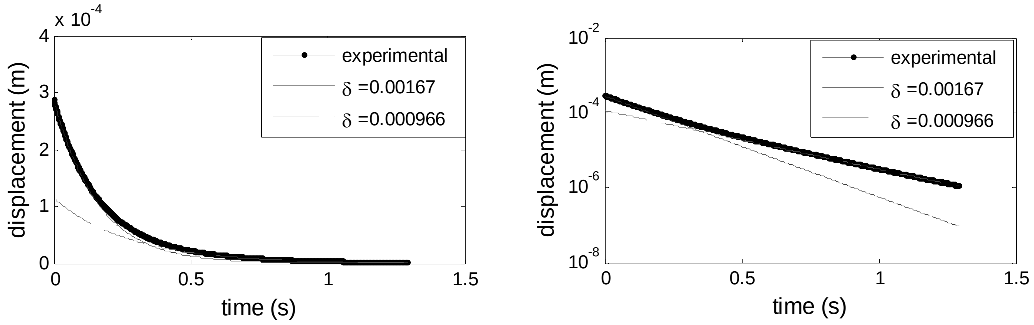

Figure 1 – Two fixed-exponential fittings of the top envelope of free vibration decay of the first natural frequency (593 Hz). The damping ratios differ by 72.8%.
a) y axis in linear scale, b) y axis in logarithmic scale.

THE METHOD OF FREE DAMPED VIBRATIONS BY TIME BLOCKS

The rate of reduction of free vibrations is typically determined using the logarithmic decrement of vibration, δ, or by the dissipation factor, ψ, the corresponding relative energy dissipation [7]. The logarithmic decrement can be related to the damping ratio, ζ, and also to the energy dissipation or damping capacity, ψ. It is determined over several (n) cycles of the decay of vibration of a single degree of freedom system from the displacement amplitudes, using

$$\delta = \frac{1}{n}\ln\frac{A_i}{A_{i+n}} = 2\pi\zeta \approx \frac{\psi}{2} \quad (1)$$

where A_i and A_{i+n} are the amplitudes corresponding to the i^{th} and the $(i+n)^{th}$ cycles of the vibrations, respectively. The damping ratio describes the decay in the time response of a linear damped single-degree-of-freedom system subjected to an initial displacement, A, as shown in equation (2),

$$x(t) = Ae^{-2\zeta\omega_n t}\cos(\omega_d t + \phi) \quad (2)$$

where ω_d is the frequency of damped free vibration, ω_n is the natural frequency and ϕ is the phase. The value of the damping ratio is the averaged characteristic of the energy dissipation in "n" cycles of the vibration.

For an amplitude-independent damping, the value of the damping ratio is unique and the classical spring mass damper system shown in equation (3) can model the vibration decay. However if the damping is amplitude-dependent, the value changes, with a different value associated with each average amplitude in the range considered, $(A_i+A_{i+n})/2$ [7]. For such cases, this amplitude dependency must be incorporated into the damping function if the dynamic behaviour of the dynamic system being considered is to be accurately modelled. One approach is to modify the damping function to directly account for amplitude dependence, as shown in the modified system of equation (4), where a linear dependence on *instantaneous* displacement is assumed. Please note that an assumption is made that the linear dependence on vibration displacement amplitude (described above and observed experimentally) will be preserved if a function of instantaneous displacement is used instead. This assumption allows generality and ease of implementation of our model.

$$\ddot{x} + 2\zeta\omega_n\dot{x} + \omega_n^2 x = 0 \quad (3)$$

$$\ddot{x} + 2(\zeta_0 + ax)\omega_n\dot{x} + \omega_n^2 x = 0 \quad (4)$$

Figure 2 shows an example experimental decay of the vibration and the lines formed by the peaks of the decays of the two single degree of freedom models of equations (3) (using a parametric 'best' fit to the experimental data). The first model (using a constant damping ratio of 0.0011) provides a good fit to the decay of vibrations but cannot follow it properly, particularly at higher amplitudes of vibration. However, the second model [equation (4)] that takes into account the dependence of the effective damping ratio on vibration displacement can be seen to follow the envelope much more precisely.

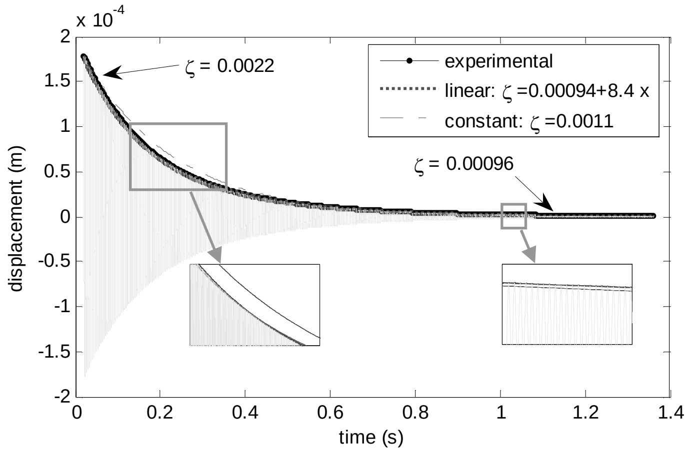

Figure 2 – Experimental free decay of vibration and the envelopes of the fittings with constant damping ratio and linearly changing damping ratio.

TEST SETUP AND EXPERIMENT

In order to apply the mechanical characteristics of the material in question to the modelling of flywheel systems, it was necessary that responses be observed for a variety of vibration amplitudes and frequencies. A relation between damping and natural frequency at low amplitude was achieved successfully in a previous paper by the authors [12], showing a constant damping for the limited range of frequencies studied. But a much wider range of frequencies had to be considered to reach the range of natural frequencies associated with a high speed flywheel system (on the order of 1 kHz). The shortest samples available to authors could practically not have a natural frequency greater than 100 Hz. Shorter beams yielded unreliable results due to end clamping effects that are difficult to control. In order to extend the measurement range, the samples were subjected to a tensile load so as to increase the effective natural frequency and, at the same time, include the effect of preload and the high levels of stress present in flywheel components. Attempts were made to use a tensile testing machine in this regard, but the clamps used to fasten the samples allowed some lateral displacement that complicated the measurement of vibration while the samples were stretched. A specially designed test rig was developed and constructed to allow stretching of the samples with a tight attachment of the clamps.

A photograph of the test setup is shown in Figure 3. The left side is fixed to the base by two large bolts and the right side can slide smoothly within the limits of the clearance between the fastening bolt and the associated hole. The desired tension is set by means of the fine pitched stretch control bolt on the far right, which pulls the sliding clamp towards a fixed block. Once the desired natural frequency for measurement is obtained, the vertical bolt is fastened, fixing the right end of the sample in that position.

The test samples are made of graphite-epoxy in a 0º-90º-0º-90ºs. They have an effective length of 110 mm and thickness of 1 mm, measured between the innermost sides of the clamp fillets. These fillets machined at each end (a dog-bone configuration), were added to minimize the effect of the friction between the sample ends and the clamps in the overall vibration decay.

Figure 3 – Test rig.

A strain gage was placed in the surface of the sample, aligned with its longitudinal axis, to determine the strain in the sample. This allowed for the calculation of the applied load (given knowledge of the Young's Modulus of the specimen) and to relate the load applied with the first natural frequency of bending vibration. A dummy strain gage was bonded to a slab of the same material as the sample, to complete a half bridge configuration, which accounts for any thermal stresses occurring in the strain gage mounted on the sample.

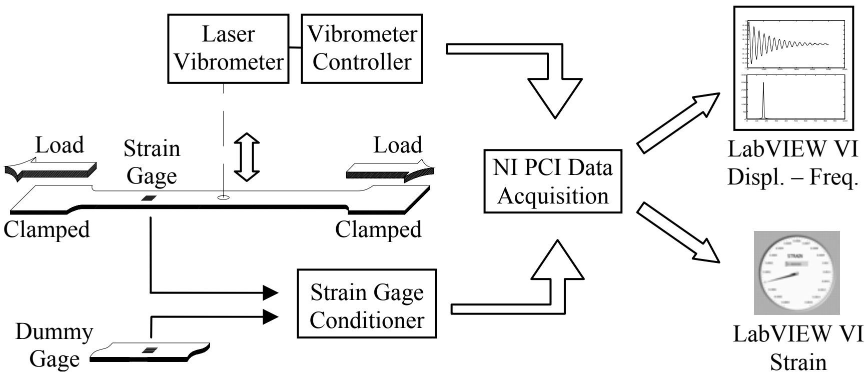

Figure 4 – Experimental setup.

The measurement procedure consisted of setting the tension of the sample, applying an initial displacement and measuring the free decay of the amplitude of vibration of the first natural frequency, using a laser vibrometer focussed on the centre of the sample. The measured signals were recorded by a computer equipped with a data acquisition system, where further signal filtering was performed to isolate the vibration at the first natural frequency from small effects coming from resonance frequencies of the rig and other natural frequencies of vibration of the beam. For the analysis of the signal, the method of free damped vibrations was applied to windows or blocks of data in the time domain. The length of each window was chosen to be of 30 cycles, i.e., including 31 peaks, after studying the correlation of results at different window sizes. This matched the criterion used in a similar study, in which 20 was determined as the minimum number of cycles to be considered for each block [2]. The sampling frequency used to register the vibration decays was 132,300 Hz. The sensitivity of the laser vibrometer was set to 80 µm/V, at which the full scale output is 1.3 mm and the resolution is 0.32 µm.

RESULTS

Similar reference amplitudes were used to measure local damping ratios in each of the time traces that were recorded. Four vibration decays were registered, at 593, 677, 735 and 744 Hz. The vibration amplitudes selected were in a range between 40 and 75 µm, which was present in all of the measured signals. The results obtained for the damping ratio show clear trends with regard to dependence on frequency and vibration. Linear functions to describe the change in damping ratio, both with respect to frequency and with respect to displacement, are a logical first candidate. As seen in Figure 5 and Figure 6, this functional form shows very good agreement with the experimentally measured results.

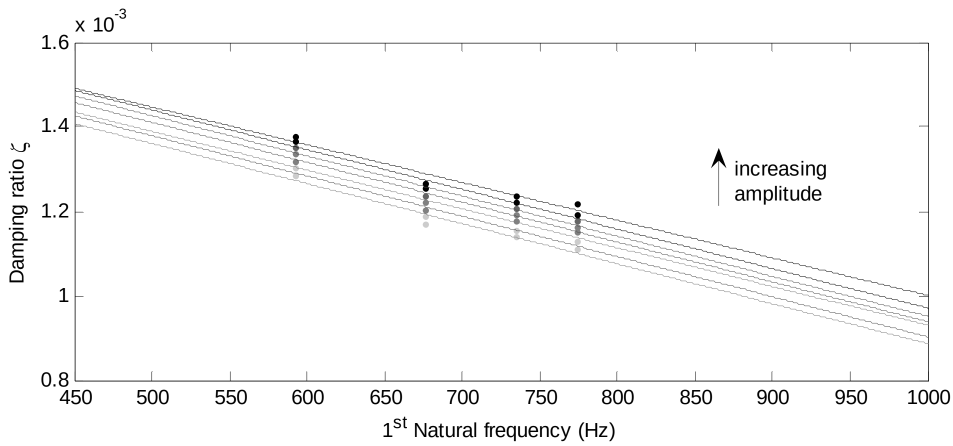

Figure 5 – Damping ratio vs. 1st natural frequency for different vibration amplitudes.

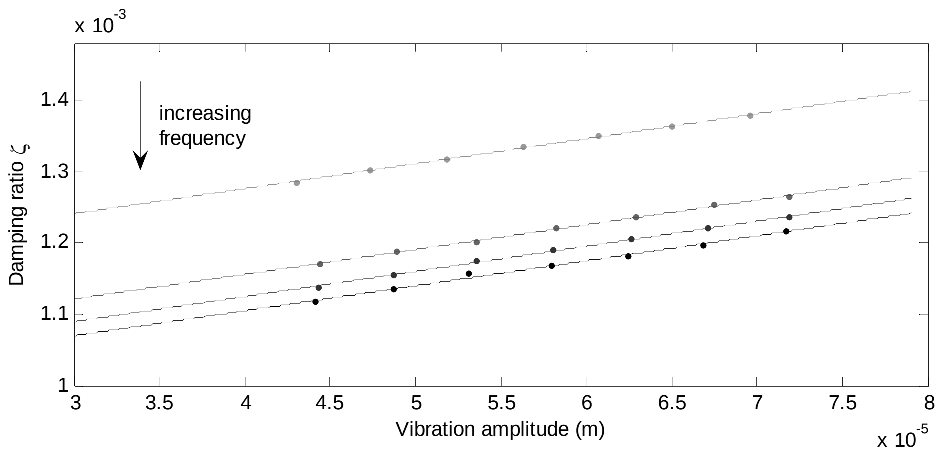

Figure 6 – Damping ratio vs. vibration amplitude for different 1st natural frequencies.

Further examination of the results showed some very interesting observations. An increase in natural frequency not also served to reduce the damping ratio, but also to increase the slope of the amplitude dependence, making a constant damping ratio even less accurate for higher frequencies. In addition for vibrations at low amplitude, a change in the natural frequency has a greater influence on the value of damping ratio. In order to account for these characteristics, the damping ratio is now modelled using four parameters. This results in the functional relation shown in equation (5), relating damping ratio, ζ, to displacement amplitude, x (in meters), and natural frequency, ω_n (in rad/s).

$$\zeta = (1.5669e\text{-}005\ \omega_n + 3.4293)\ x + (-1.5083e\text{-}007\ \omega_n + 0.0016837) \qquad (5)$$

CONCLUSIONS

A detailed study of the damping characteristics of carbon-epoxy composite components has been conducted. This has included both experimental testing of composite samples and model development. Vibration amplitude and frequency was shown to have a substantial influence on the effective damping ratios.

A correlation between the measured damping ratios for different frequencies and amplitudes has resulted in the development of a model for damping ratio that is described using linear functions of frequency and amplitude. This model provides increased predictive accuracy as compared using a constant damping ratio. As the natural frequency increases, the damping ratio becomes smaller and the dependence of damping ratio on amplitude becomes more pronounced. The model proposed can clearly simulate the experimental results in a more precise fashion and is consistent throughout the range of natural frequencies studied.

REFERENCES

[1] Gowayed Y., Abdel-Hady F., Flowers G.T., Trudell J., "Optimal Design of Multi-direction Composite Flywheel Rotors", *Polymer Composites*. **23**(3), 433-441 (June 2002).

[2] Kinra V.K., Ray S., Zhu C., Friend, Rawal S. P., "Measurement of Nonlinear Damping in a Gr/Al Metal-Matrix Composite", *Experimental Mechanics*, **37**(1), 5-10 (Mar 1997).

[3] Gibson R.F., "Dynamic Mechanical Properties of Advanced Composite Materials and Structures: A Review of Recent Research", The Shock and Vibration Digest, **22**(8), 3-12 (Aug 1990).

[4] Gibson R.F., "Dynamic Mechanical Properties of Advanced Composite Materials and Structures: A Review", The Shock and Vibration Digest, **19**(7), 13-22 (July 1987).

[5] Ewins D.J., *Modal Testing: Theory, Practice and Application*, (Research Studies Press LTD, Baldock, England, 2000).

[6] Gibson R.F., *Principles of Composite Material Mechanics*, (McGraw Hill Inc., 1994).

[7] Zinoviev P.A., Ermakov Y.N, *Energy Dissipation in Composite Materials*, (Technomic Publishing Company Inc., 1994).

[8] Suarez S.A., Gibson R.F., Sun C.T., Chaturvedi S.K., “The Influence of Fiber Length and Fiber Orientation on Damping and Stiffness of Polymer Composite Materials”, Experimental Mechanics, **26**(2) , 175-184 (1986).

[9] Sun C.T., Wu J.K. and Gibson R.F., “Prediction of material damping of laminated polymer matrix composites”, Journal of Materials Science, **22**(3), 1006-1012 (1987).

[10] Ungar E.E, Kerwin E.M Jr., “Loss Factors of Viscoelastic Systems in Terms of Energy Concepts”, J. Acoust. Soc. Am, **34**(7), 954-957 (July 1962).

[11] Chen J., Gowayed Y., Moreira A. and Flowers G., “Damping of Polymer Composite Materials for Flywheel Applications”, *Polymer composites*, **26** (2005).

[12] Moreira A., Flowers G.T., and Gowayed Y., “Effects of Internal Damping on the Dynamic Stability of High-Speed Composite Rotor Systems”, ICSV 10 (2003).

[13] Linacre E., “Damping Capacity, Part II-Effects of Conditions of Measurement”, Iron and Steel, 285-286 (June 1950).

[14] Linacre E., “Damping Capacity, Part I: Introduction and Technique of Measurement”, Iron and Steel, 153-156 (May 1950).

[15] Wallace M., Bert C., “Experimental Determination Of Dynamic Young's Modulus And Damping Of An Aramid-Fabric/Polyester Composite Material”, Proc. Okla. Acad. Sci, 59:98-101 (1979).

[16] Cloud C.H., Maslen E.H., Barret L.E., “Evaluation of Damping Ratio Estimation Techniques for Rotordynamic Stability Measurements”, Proc. IMechE, 541-550, (2004).

[17] Wettergren H.L., *Rotordynamic Analysis with Special Reference to Composite Rotors and Internal Damping*. (Doctoral Thesis, Linkoping University, 1996).

[18] Beranek L.L., Ver I.L., *Noise and Vibration Control Engineering*, (John Wiley and Sons, 1992).